IMECE2011-64425

THEORETICAL ANALYSIS ON FILM THICKNESS OF INTERTUBE FALLING-FILM FLOW WITH A COUNTERCURRENT GAS FLOW

Binglu RUAN [1, 2]   **Huan LI** [3],   **Qiuwang WANG** [2]

[1] Department of Thermal Engineering, Tsinghua University, Beijing, PR of China, 100084
[2] School of Energy and Power Engineering, Xi'an Jiaotong University, Xi'an, PR of China, 710049
[3] Mechanical Science and Engineering, University of Illinois, Urbana, IL, USA, 61801

ABSTRACT

In falling–film type of heat exchangers, gas/vapor usually exists, and its effect on falling-film mode transitions and heat transfer could not be neglected. It could impact the film thickness, which is an important parameter to determine the thin-film heat transfer performance, or even destroy falling-film modes and significantly deteriorate the heat transfer. However, there have been very few studies of countercurrent gas flow effects on the film thickness. In this paper, the falling-film film thickness with and without liquid-gas interfacial shear stress due to the countercurrent gas flow was studied. A two-phase empirical correlation is used to solve the momentum equation. Calculation results were compared with available experimental data in literatures for validation. Reasonable agreement was achieved. Thus, the two-phase correlation for predicting shear stress of a thin film flow inside a vertical rectangular channel has been extended to a new type of flow. Effects of film Reynolds number, gas velocity, and gas-channel equivalent hydraulic diameter on the film thickness were studied. It is shown that the countercurrent gas flow thickened the falling film. The increased film thickness can shift the mode transitional Reynolds number and reduce the heat transfer coefficient, corroborating the conjecture in our earlier work.

Keywords: falling-film, film thickness, countercurrent, two-phase flow, gas flow effects

1. INTRODUCTION

Compared to conventional flooded bundle heat exchangers, horizontal-tube falling-film heat exchangers have many advantages: higher heat transfer coefficient, lower liquid inventory, smaller volume, better oil return and reduced manufacture cost *et al.* [1]. Hence, they have been introduced in chemical Engineering, refrigeration, petroleum refining, paper-making, desalination and food industries for energy conservation and environmental protection, as evaporators, condensers, absorbers, and evaporative coolers *et al.*

For a thin film flow, film thickness is a vital factor to determine its heat transfer performance. If the film is too thick, thermal resistance of the film would be large and the heat transfer coefficient could be reduced; if the film is too thin, local "dryout" may happen and sharply reduce the heat transfer coefficient [2]. Many investigators have explored the film thickness and its effect on heat transfer of the falling-film flow with a vertical or horizontal plate [3-5]. However, heat transfer of a falling-film flow with a vertical or a horizontal plate is quite different from that of a falling-film flow around a horizontal tube, due to their different liquid-solid interfacial shapes. When a falling liquid flowing around a horizontal tube, the flow can be divided into the stagnation region, the jet impingement region, the thermal developing region and the fully developed region according to the dynamic and thermal behaviors of the film circumferentially from the top to the bottom of the tube [6]. The film thickness varies in different region, and different heat transfer coefficient can be observed [7, 8]. Falling-film film thickness around a horizontal tube has been explored experimentally by several investigators. Gstoehl *et al.* [9] developed a new laser technique to measure the film thickness of water, ethylene glycol and the water-glycol mixture. They obtained a good agreement with the Nusselt theory at the top of the tube. Xu *et al.* [10] investigated the film thickness of water and stated that the film thickness and its distribution around the tube can be affected by the feeding flow rate, the tube diameter and the circumferential angle of the tube.

However, few researches on gas flow effects on falling-film film thickness around a horizontal tube could be found in open literatures. In falling-film heat exchangers, vapor usually exists and its effect on mode transitions and heat transfer could

1   Copyright © 2011 by ASME

not be neglected. According to our previous work, existence of vapor can shift the transitional Reynolds number [11], or even destroy the falling-film modes, and finally impact the heat transfer. One of the conjectures made in our previous work [11] is that a countercurrent gas flow could thicken the film thickness and lead to a decreased transitional *Re* with an increased gas velocity. The effect will be theoretically analyzed in this paper, and some parametric studies will be carried out.
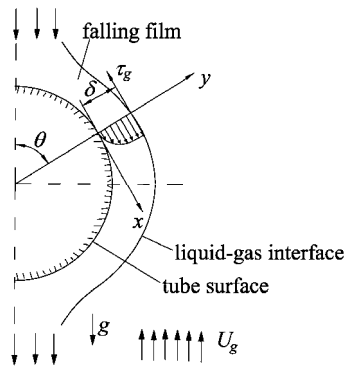
2. MATHEMATICAL ANALYSIS

Fig.1 a falling liquid film flowing around a horizontal tube

Fig.1 shows the schematic diagram of the mathematical model. The falling film goes downward and flows around a horizontal tube with circumferential angle of θ and film thickness of δ. Several assumptions are made to simplify the calculation: the falling-film flow is two-dimensional, laminar, steady and non-compressible; the whole surface of the tube is covered by the liquid film; the liquid film is non-wavy and smooth; the fluid properties are constant; the inertial force of the falling film is neglected; the viscous force at the liquid-gas interface is neglected; the pressure gradient in *x* direction is neglected.

2.1 Case A: falling-film flow in a quiescent surrounding

Based on the assumptions made above, the momentum equation of the falling liquid film can be expressed as

$$\mu \frac{\partial^2 u}{\partial y^2} = -\rho g \sin\theta , \qquad (1)$$

where μ is the dynamic viscosity of the liquid, u is the velocity of the falling film, ρ is the density of the liquid and g is the gravity acceleration.

Integrating Eq. (1), and applying the zero-viscous-force boundary condition at the liquid-gas interface

$$\left. \frac{\partial u}{\partial y} \right|_{y=\delta} = 0 , \qquad (2)$$

Eq. (1) becomes

$$\frac{\partial u}{\partial y} = -\frac{\rho g \sin\theta}{\mu} y + \frac{\rho g \sin\theta \delta}{\mu} . \qquad (3)$$

Integrating Eq. (3) and applying the non-slip boundary condition at the tube surface, $u|_{y=0} = 0$, the velocity profile can be defined by

$$u(y) = \frac{\rho g \sin\theta}{\mu} \left(\delta y - \frac{y^2}{2} \right) . \qquad (4)$$

The average velocity of the liquid film, $\overline{U}$, can be calculated as

$$\overline{U} = \frac{1}{\delta} \int_0^\delta u(y)\, \mathrm{d}y = \frac{\rho g \sin\theta \delta^2}{3\mu} . \qquad (5)$$

The mass flow rate per unit length of the falling liquid film, Γ, is defined as

$$\Gamma = 2 \cdot \rho \cdot \overline{U} \cdot \delta . \qquad (6)$$

The film Reynolds number can be obtained as

$$Re = \frac{2\Gamma}{\mu} = \frac{4\rho^2 g \sin\theta \delta^3}{3\mu^2} . \qquad (7)$$

Hence, the falling-film thickness, δ, can be calculated by Eq. (5) and Eq. (6) as

$$\delta = \left(\frac{3\Gamma\mu}{2\rho^2 g \sin\theta} \right)^{1/3} . \qquad (8)$$

Eq. (8) can also be written as a function of the film *Re* by

$$\delta = \left(\frac{3\mu^2 Re}{4\rho^2 g \sin\theta} \right)^{1/3} . \qquad (9)$$

Hence, if the mass flow rate per unit length and the feeding Reynolds number is known, the thickness can be easily obtained. It is noted in Eq. (8) and Eq. (9) that, as θ approaches 0º or 180º, the calculated δ will be infinite. Calculation is not valid and should be avoided in these regions.

2.2 Case B: falling-film flow with a countercurrent gas flow imposed

When a countercurrent gas flow imposed on the falling film, the flow condition may behave differently with different gas velocities. If the gas velocity is small, the falling- film flow is stable; with an increased gas velocity, the flow behaves more and more unstable. It is found in our previous work that when the gas velocity U_g was larger than 3.5m/s, the falling water film became unstable [11]. With further increase of the gas velocity, flooding may occur [12]. This work mainly focused on how countercurrent gas flow thickens the falling-film film thickness. Hence, no flooding or unstable effects were considered.

With assumptions made earlier, the governing equations of the falling film can be given as

$$\mu \frac{\partial^2 u}{\partial y^2} = -\rho g \sin\theta \cdot \tag{10}$$

Integrating Eq. (10) twice, and applying the non-slip boundary condition at the tube surface, $u|_{y=0} = 0$, and the shear stress, τ_i, boundary condition at the liquid-gas interface, $\left.\frac{\partial u}{\partial y}\right|_{y=\delta} = \frac{\tau_i}{\mu}$, Eq.(10) becomes

$$u(y) = -\frac{\rho g \sin\theta}{2\mu} y^2 + \frac{\rho g \sin\theta\delta + \tau_i}{\mu} y \cdot \tag{11}$$

The average velocity of the liquid film, $\overline{U}$, can be obtained as

$$\overline{U} = \frac{1}{\delta}\int_0^\delta u(y)\,\mathrm{d}y = \frac{\rho g \sin\theta\delta^2}{3\mu} + \frac{\tau_i\delta}{2\mu} \cdot \tag{12}$$

With Eq. (6) and Eq. (12), the film Reynolds number with gas shear can be expressed by

$$Re = \frac{2\Gamma}{\mu} = \frac{4\rho^2 g \sin\theta\delta^3}{3\mu^2} + \frac{2\rho\delta^2\tau_i}{\mu^2} \cdot \tag{13}$$

Denote the film Reynolds number in quiescent surroundings as Re_A, and the corresponding film thickness as δ_A, while the film Reynolds number with a countercurrent gas flow as Re_B, and the corresponding film thickness as δ_B. Suppose the feeding Reynolds numbers were the same for case A and case B, by comparing Eq. (7) and Eq. (13), the relation between δ_A and δ_B can be expressed as

$$\delta_2 = \left(\delta_1^3 - \frac{3\delta_2^2\tau_i}{2\rho g \sin\theta}\right)^{1/3}, \tag{14}$$

where $\tau_i < 0$ for a countercurrent gas flow. Hence, when a countercurrent gas flow is imposed on a falling liquid flow, the film thickness always increases. Increased film thickness could lead to an increased local mass of the liquid at the bottom of the stabilizing tube, and induce a "late" falling film mode transition from sheet mode to jet mode with an decreased feeding mass flow rate and an "earlier" transitions from jet mode to sheet mode with an increased feeding mass flow rate, comparing to those without gas flow imposed. Hence, it is observed in our previous work [11] that the transitional Reynolds numbers between jets and sheets were decreased when a countercurrent gas flow was imposed.

Several models were proposed by researchers to calculate the liquid-gas interface shear stress τ_i independently. Blasius' equations were used to calculated the shear stress when liquid and gas flow in the same direction [13]. To calculate the shear stress of a falling-film flow inside a vertical rectangular channel with a countercurrent gas flow, Drosos et al. [12] employed the empirical correlations proposed by Bharathan et al. [14] for the same type of flow. To the authors' knowledge, there are no data

or model available for calculating the interfacial shear stress of a falling film flow with a countercurrent gas imposed in open literatures. Hence, the model proposed by Bharathan et al. [14] may be used as well in this work to estimate the τ_i of a similar flow:

$$\tau_i = -\frac{1}{2} f_i \rho_g \left(U_g + U_1\right)^2 \tag{15}$$

$$f_i = 0.008\left[1 + C_1\left(\frac{\delta_A}{D}\right)^{C_2}\right] \tag{16}$$

$$C_1 = 41.3 Bo^{(C_2+0.25)} 10^{9.07/Bo} \tag{17}$$

$$C_2 = 1.63 + \frac{4.74}{Bo} \tag{18}$$

$$Bo = D\left[\frac{(\rho - \rho_g)g}{\sigma}\right]^{0.5} \tag{19}$$

where f_i is the friction coefficient of the liquid-gas interface; ρ_g is the density of the gas; U_g is the velocity of gas phase; U_1 is the velocity of liquid phase, and it is equal to $\overline{U}$ in Eq. (12) for convenience; δ_A is the film thickness in quiescent surroundings; σ is the surface tension of the liquid; D is the equivalent hydraulic diameter of the gas flow channel. Fig.2 shows the schematic diagram of the calculation parameters of the equivalent hydraulic diameter, D, which can be obtained by

$$D = \frac{4A}{P} = 4(a - r\sin\theta) \cdot \tag{20}$$

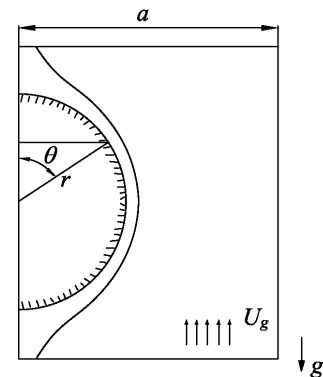Bo is the modified Bond number based on D.

Fig.2 schematic diagram of the equivalent hydraulic diameter calculation

Consider a special case that the gas velocity is increased and flooding is about to occur. By applying the non-slip

boundary condition at the tube surface, $u|_{y=0} = 0$, and the liquid zero-velocity boundary condition at the liquid-gas interface, $u|_{y=\delta} = 0$, to Eq. (10), the critical flooding film thickness, δ_c, can be easily obtained as

$$\delta_c = \left(\frac{3\mu^2 Re}{\rho^2 g \sin\theta} \right)^{1/3} . \qquad (21)$$

By denoting the film thickness in quiescent surroundings as δ_A, and comparing Eq. (21) to Eq. (9), the relation between δ_A and δ_c can be given as

$$\delta_c = 1.587\delta_A . \qquad (22)$$

3. RESULTS AND DISCUSSION

3.1 Case A: falling-film flow in a quiescent surrounding

Calculated results for falling water film without gas flow are compared with experimental data reported by Gstoehl et al. [9] for validation in Fig.3. The film thicknesses are plotted against the circumferential angle θ in Fig.3. The Re is 574, which is set to be the same as the experimental Re stated by Gstoehl et al. [9]. It can be seen in Fig.3 that, for θ within the range of 20º~80º, the calculated results agrees well with the experimental data, with an average deviation of 6.6%. For θ within the range of 110º~140º, the average deviation is around 8.7%. When θ is larger than 140º, deviation between the calculation results and the experimental data increases significantly. This may be due to the assumption of neglect of inertial force of the film flow made earlier.

Calculated film thicknesses are also compared with the experimental data presented by Xu et al. [10] at different mass flow rate per unit length in Fig.4. The calculation results agrees well with experimental data of Xu et al. [10] when Γ is
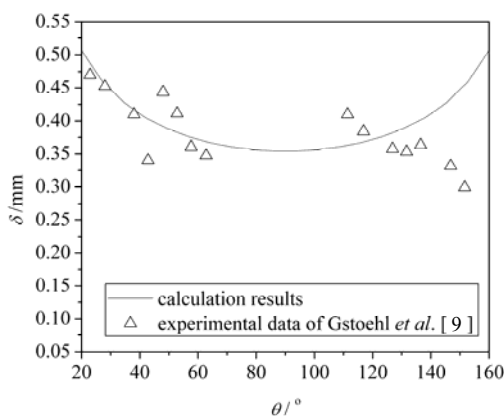

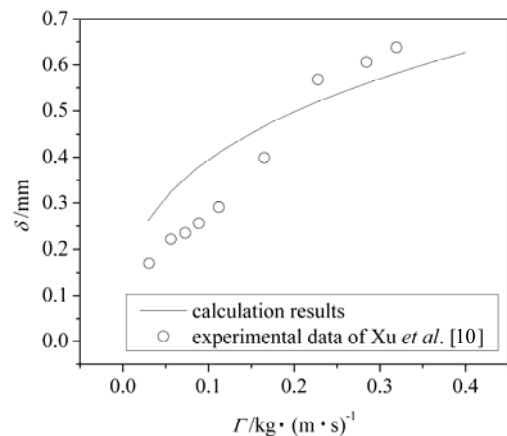Fig.3 circumference distribution of falling film thickness on a horizontal tube (Re=574)

Fig.4 falling film thickness variation with mass flow rate per unite length, Γ, (θ=90º)

larger than 0.2, with an average deviation of 8.3%. When Γ is smaller than 0.2, the average deviation becomes larger.

With an increasing Re, falling film modes of droplets, jets and sheets will appear. These modes can be observed between horizontal tubes. However, depending on the falling-film modes, the film thickness can be uniform or nonuniform in axial direction of the tube due to Taylor instability. If sheet mode appears, the film thickness can be evenly distributed; if droplet mode or jet mode appears, at a fixed circumferential angle, the film thickness along the length of the tube will be uneven. In this work, the nonuniform distribution of the film thickness due to the Taylor instability is neglected, and the film thickness variation with circumferential angle at different Re is plotted in Fig.5. Due to the neglect of surface tension effect and inertial force of the film flow, the film thickness distributes symmetrically above and below the horizontal center-line of the tube (θ=90º). Fig.6 shows the falling film thickness plotted against Re at different circumferential angle, θ. The film thickness increased with the increased feeding Re nonlinearly. Moreover, the decrease of δ with an increased θ at a small Re is not as significant as that at a larger Re.
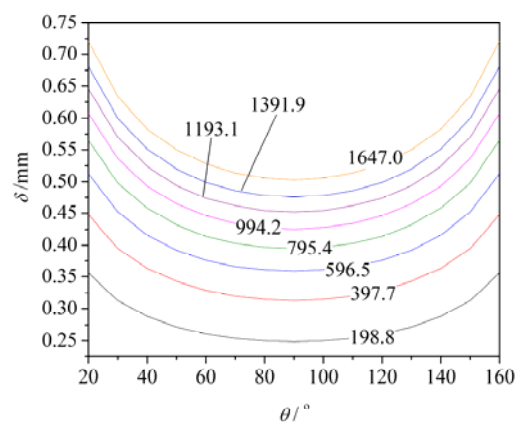

Fig.5 circumference distribution of falling film thickness on horizontal tube at different Re
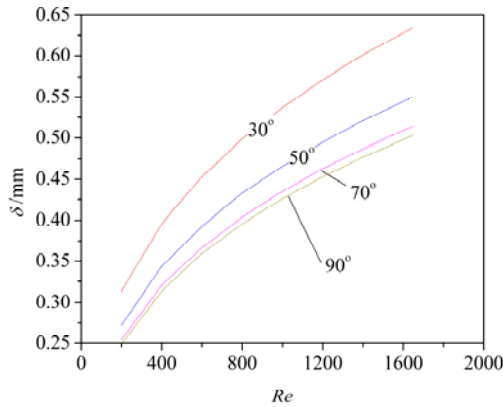
4   Copyright © 2011 by ASME

Fig.6 falling film thickness variation with feeding Re at different circumferential angle of horizontal tube

3.2 Case B: falling-film flow with a countercurrent gas flow imposed

To the author's best knowledge, there is no experimental data available for the falling-film film thickness around a horizontal tube with a countercurrent gas flow in open literatures. However, Drosos et al. [12] explored countercurrent gas flow effects on the thickness of falling film flowing inside a vertical channel. The data reported by Drosos et al. [12] may be employed to compare with our theoretically calculated results when θ=90°. Table 1 shows the value of parameters used in the calculation. Fig.7 shows the film thickness plotted against the gas velocity at θ=90°. It is observed in Fig.7 that the experimental data is over-predicted by the model by around 47%. However, the calculated film-thickness variation trend agrees well with the experimental data. The deviation may be induced by different types of the falling-film flow. Though the calculated results at position of θ=90° are adopted to compare with the experimental data presented by Drosos et al. [12], it should be noted that the film thickness at θ<90° can have effects on that at θ=90°. For a falling film flowing around a horizontal tube, since the gravity acceleration, $g\sin\theta$, is always less than the gravity acceleration of a falling film in a vertical channel, g, at θ<90°, the film thickness of the falling-film flowing around a horizontal tube should be larger than that in a vertical channel at θ=90°. Moreover, Drosos et al. [12] reported that the critical flooding gas-velocity was 8.8 m/s at Re=620 for falling-film flowing in a vertical channel. By using Eq. (21), the critical flooding film-thickness can be obtained at the same Re as 0.5774 mm, and the corresponding critical flooding gas-velocity can be estimated as 7.8 m/s for the flow around a horizontal tube. The deviation between the two critical gas velocities is 11.4%. Hence, it may be concluded that our calculation can estimate the film thickness of a falling film flowing around a horizontal tube reasonably.

Table 1 value of parameters in calculation

Re	ρ kg·m^{-3}	μ kg·(m·s)$^{-1}$	ρ_g kg·m^{-3}	σ N·m^{-1}	a m	r m
620	998.2	1.004×10^{-3}	1.2	0.072	0.02	1.27×10^{-2}

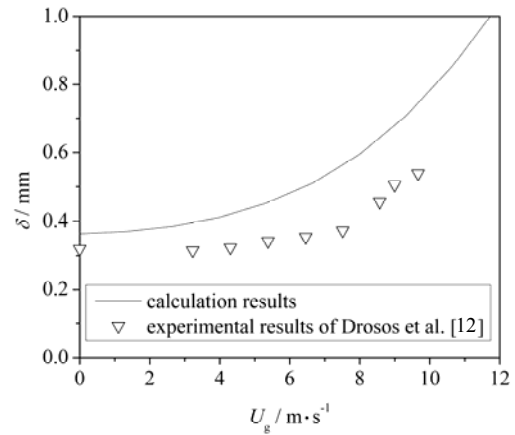Fig.7 falling film thickness variation with gas velocity at θ=90°, Re=620

By neglecting the flooding and the axially nonuniform induced by Taylor instability, the film thickness variation with countercurrent gas velocity for different Re at θ=90° is plotted in Fig.8. It is shown in Fig.8 that the film thickness increases with the gas velocity nonlinearly. With an increasing U_g, the slop of the curve increases. Fig.9 shows the film thickness plotted against the feeding Reynolds number at different gas velocity. It is observed that the film thickness increases with an increased Re, and the variation is more significant when the gas velocity is large.

Fig.10 shows the film thickness plotted against gas velocity at different circumferential angle for a small and a large Re. Fig. 11 shows the film thickness plotted against the circumferential angle at different gas velocity for Re=198.8 and Re=994.2. It is shown in Fig.10 that with an increased gas
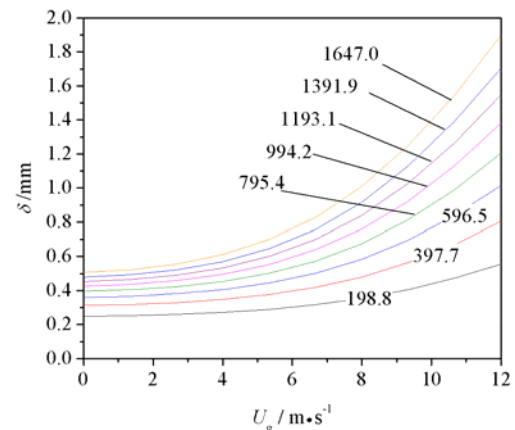

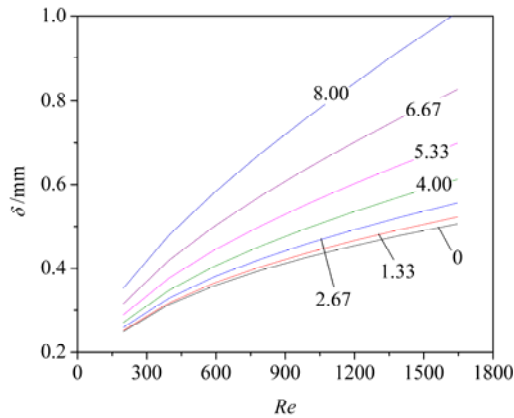Fig.8 falling-film thickness variation with the gas velocity at different Re, θ=90°

5   Copyright © 2011 by ASME

Fig.9 falling-film thickness variation with the feeding Re with different countercurrent gas velocity imposed, θ=90°
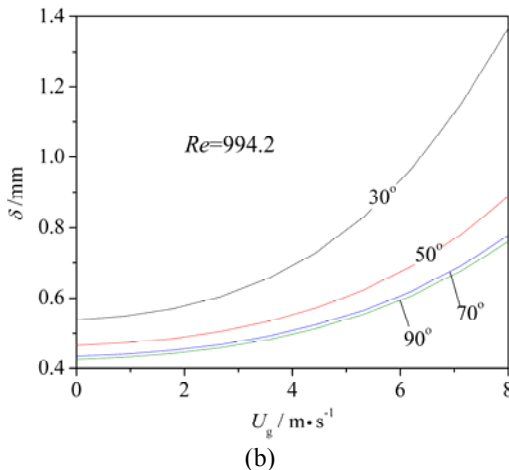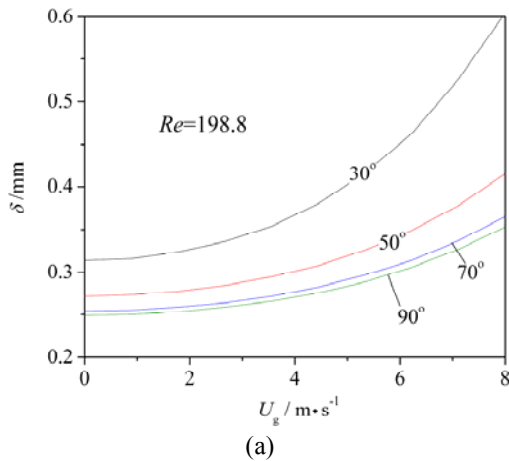

(a)

(b)

Fig.10 falling-film thickness variation with the gas velocity at different circumferential angle: (a) Re=198.8; (b) Re=994.2

velocity, the film thickness increases at different circumferential angle. The film thickness increase is more significant at a small circumferential angle than that at a large circumferential angle

when θ<90°. For Re=994.2, the film thickness increases around 75% at θ=30° with U_g increased from 0 m/s to 6 m/s. By comparing the film thickness increase at a fixed circumferential angle in Fig.11, it can be seen that with an increased gas velocity, the film thickness increase becomes obvious. Especially when θ approach 20°, the film thickness increase can reach up to 16% for the gas velocity increase from 4 m/s to 5 m/s.
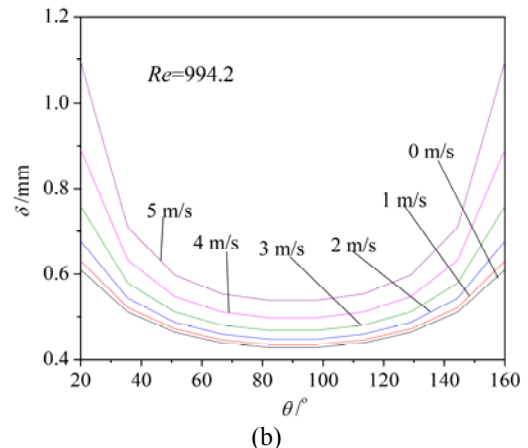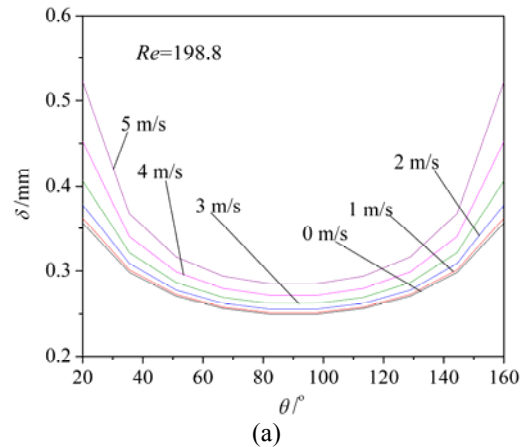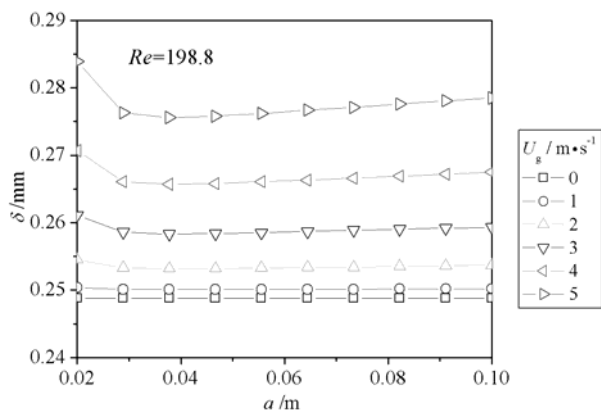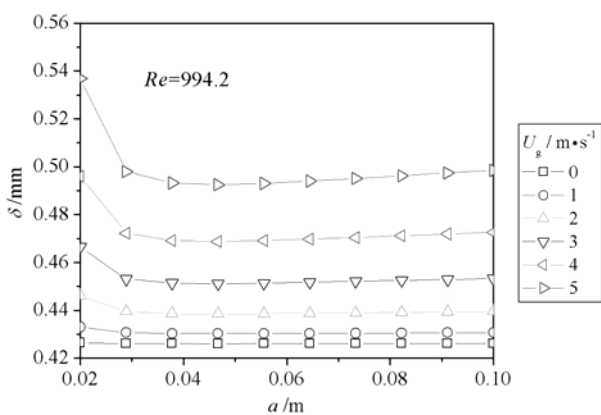

(a)

(b)

Fig.11 falling-film thickness variation with circumferential angle with different countercurrent-gas velocity: (a) Re=198.8; (b) Re=994.2

Fig.12 shows the film thickness plotted against the gas-channel width, a (see definition of a in Fig.2), at different gas velocities for a lower Reynolds number, 198.8, and a higher Reynolds number, 994.2. Since $a=D/4+r$, the effects of a can be regarded as the effects of the gas-channel equivalent hydraulic diameter D. It is shown in Fig.12 that the gas-channel-width effect is not significant when U_g is small. However, the film thickness decreases sharply and then increases gradually when U_g is larger than 2 m/s. The minimum film thickness can be observed at $a \approx 37$mm. The slight increase of the film thickness at a>37mm may be due to the pressure decrease of the gas with an increased width of the channel.

6   Copyright © 2011 by ASME

(a)

(b)

Fig.12 falling-film thickness variation with width of
countercurrent gas-channel at different gas velocity (θ=90°):
(a) Re=198.8; (b) Re=994.2

4. CONCLUSIONS

Countercurrent gas flow effects on the falling-film thickness around a horizontal tube were analyzed theoretically. An empirical correlation was employed to calculate the shear stress at the liquid-gas interface. Film thickness with and without a countercurrent gas flow effects was calculated. The results were compared with experimental data of a similar falling-film flow presented in literatures. Effects of the feeding Reynolds number, circumferential angle, gas velocity and gas-channel width (gas-channel equivalent hydraulic diameter) were explored. Conclusions can be summarized as: the film thickness increased with an increased Reynolds number and gas velocity; decreased with an increased circumferential angle when the angle is less than 90°; and decreased firstly and then increased slightly with an increased gas-channel equivalent hydraulic diameter when Re is large. Because there is virtually no experimental data or model currently available in the literature to predict these effects for a falling film flowing around a horizontal tube, there is significant value in providing a mathematical tool to estimate them. Such a tool provides a starting point for our further experimental work in this direction and may provide some engineering guidance.

REFERENCES

[1] Ribatski, G., and Jacobi, A. M., 2005, "Falling-Film Evaporation on Horizontal Tubes - a Critical Review," International Journal of Refrigeration, 28(5), pp. 635-653.

[2] Ribatski, G., and Thome, J. R., 2007, "Experimental Study on the Onset of Local Dryout in an Evaporating Falling Film on Horizontal Plain Tubes," Experimental Thermal and Fluid Science, 31(6), pp. 483-493.

[3] Portalski, S., 1963, "Studies of Falling Liquid Film Flow - Film Thickness on a Smooth Vertical Plate," Chemical Engineering Science, 18(12), pp. 787

[4] Zhou, D. W., Gambaryan-Roisman, T., and Stephan, P., 2009, "Measurement of Water Falling Film Thickness to Flat Plate Using Confocal Chromatic Sensoring Technique," Experimental Thermal and Fluid Science, 33(2), pp. 273-283.

[5] Zaitsev, D. V., and Kabov, O. A., 2005, "Study of the Thermocapillary Effect on a Wavy Falling Film Using a Fiber Optical Thickness Probe," Experiments in Fluids, 39(4), pp. 712-721.

[6] Chyu, M. C., and Bergles, A. E., 1987, "An Analytical and Experimental-Study of Falling-Film Evaporation on a Horizontal Tube," Journal of Heat Transfer-Transactions of the ASME, 109(4), pp. 983-990.

[7] Rogers, J. T., 1981, "Laminar Falling Film Flow and Heat-Transfer Characteristics on Horizontal Tubes," Canadian Journal of Chemical Engineering, 59(2), pp. 213-222.

[8] Hu, X., and Jacobi, A. M., 1996, "The Intertube Falling Film .2. Mode Effects on Sensible Heat Transfer to a Falling Liquid Film," Journal of Heat Transfer-Transactions of the ASME, 118(3), pp. 626-633.

[9] Gstoehl, D., Roques, J. F., Crisinel, P., and Thome, J. R., 2004, "Measurement of Falling Film Thickness around a Horizontal Tube Using a Laser Measurement Technique," Heat Transfer Engineering, 25(8), pp. 28-34.

[10] Xu, L., Wang, S. C., Wang, Y. X., and Ling, Y., 2003, "Flowing State in Liquid Films over Horizontal Tubes," Desalination, 156(1-3), pp. 101-107.

[11] Ruan, B., Jacobi, A. M., and Li, L., 2009, "Effects of a Countercurrent Gas Flow on Falling-Film Mode Transitions between Horizontal Tubes," Experimental Thermal and Fluid Science, 33(8), pp. 1216 -1225.

[12] Drosos, E. I. P., Paras, S. V., and Karabelas, A. J., 2006, "Counter-Current Gas-Liquid Flow in a Vertical Narrow Channel-Liquid Film Characteristics and Flooding Phenomena," International Journal of Multiphase Flow, 32, pp. 51-81.

[13] Brauner, N., Moalem Maron, D., and Rovinsky, J., 1998, "A Two-Fluid Model for Stratified Flows with Curved Interfaces," International Journal of Multiphase Flow, 24, pp. 975-1004.

[14] Bharathan, D., Wallis, G. B., and Richter, H. J., 1979, "Air-Water Counter-Current Two-Phase Flow," EPRI Rep., NP-1165.